Available online at www.sciencedirect.com

jmr&t
Journal of Materials Research and Technology

journal homepage: www.elsevier.com/locate/jmrt

Damage characterisation of amine-functionalized MWCNT reinforced carbon/epoxy composites under indentation loading

Usaid Ahmed Shakil [a,b,*], *Mohd Ruzaimi Mat Rejab* [c], *Norazlianie Sazali* [d], *Shukur Abu Hassan* [a,b], *Mohd Yazid Yahya* [a,b], *Quanjin Ma* [c]

[a] *Centre for Advanced Composite Materials (CACM), Universiti Teknologi Malaysia, Johor Bahru, 81310, Malaysia*
[b] *School of Mechanical Engineering, Universiti Teknologi Malaysia, Johor Bahru, 81310, Malaysia*
[c] *Faculty of Mechanical and Automotive Engineering Technology, Universiti Malaysia Pahang, Pekan, 26600, Malaysia*
[d] *Centre of Excellence for Advanced Research in Fluid Flow (CARIFF), Universiti Malaysia Pahang, Gambang, 26300, Malaysia*

ARTICLE INFO

Article history:
Received 13 January 2023
Accepted 27 April 2023
Available online 29 April 2023

Keywords:
Damage resistance
Fibre reinforced nanocomposites
Amine-functionalized MWCNT
Quasi-static indentation
Non-destructive inspection
Toughness mechanisms

ABSTRACT

Damage resistance of carbon fibre reinforced composites is crucial parameter to be considered at both primary selection and in-service maintenance stages. High stiffness of carbon-epoxy system and stacked configuration make it susceptible to impact induced brittle damages. Delamination is one such life-limiting damage modes that can severely inhibit load carrying capacity of laminates. Hence to improve the damage resistance of composites demands tailoring tough microstructure and altering brittle damage modes with ductile ones. This work attempted to design damage resistant carbon composites through modification of epoxy matrix with amine functionalized multi walled carbon nanotubes (NH_2-MWCNT). Laminates with different nanotube concentrations (0.3, 0.6, 0.9 and 1.2 wt. %) were fabricated to investigate its influence on load bearing capacity, toughness and damage resistance of fibre reinforced nanocomposites. Generally, peak force, displacement and toughness until maximum force improved at all nanoparticle concentrations. Matrix cracking was suppressed owing to optimum cross-linking of nanoparticle with matrix. External damage area increased with nanoparticle concentration although delaminated area, mapped through c-scan, was suppressed up to 27.73%. A combination of higher degree of interfacial interactions, induced by nanoparticles, and energy absorbing microstructure was concluded to be behind improvement in the damage resistance of composites.

* Corresponding author.
E-mail address: usaid.ahmed98@gmail.com (U.A. Shakil).

https://doi.org/10.1016/j.jmrt.2023.04.242

1. Introduction

Fibre reinforced composites have successfully gained niche in structural material's market, in the last few decades, owing to their exceptional mechanical properties, durability and lightweight characteristics. Their usage as load bearing components and structures can be discerned from the variety of application areas including automotive, aerospace, and civil construction sectors. A wide variety of fibre and resin systems allow optimizing cost and strength requirement together with tailoring responses of the resulting composites. This flexibility has assisted composites in replacing conventional structural materials such as steel, aluminium and titanium [1].

Laminated composites exhibit superior performance due to synergistic properties of constituent materials i.e., fibre and matrix. A third constituent is interface that is responsible for transferring load from matrix to fibres. A trade-off between toughness and strength is inevitable depending upon how strong the interface is. Stronger interface offers strength and stiffness to composites whereas weaker interface induces high resistance to fracture [1]. Much of the research effort have been devoted to optimizing these properties in laminated composites [2,3]. A besetting issue with composites is delamination that stems from the stacked configuration of fibre layers. Laminated composites feature a resin-rich interlaminar region that often serves as crack initiation and propagation plane under external loading [4]. Incipient interlaminar cracks either can migrate towards adjacent fibre layers or propagate unstably within interlaminar zone [5]. Both scenarios directly influence load bearing capacity of composites either by causing fibre-matrix interface failure, through crack migration, or deteriorating cohesive response of laminates, through interlaminar debonding.

Interlaminar damages have been reported to be especially sensitive to out of plane loading. Since properties in transverse direction are controlled, primarily, by matrix, significant volume of research has focused on characterising damages in composites due to external transverse loading [6,7]. The most common of such loading type in in-service condition is projectile impact. A variety of techniques has been established to simulate projectile impact conditions including ballistic impact, low-velocity impact and quasi-static indentation test. Advantage of indentation test lies in singling out damage events and sequence on force–displacement curves though neglecting strain rate effect. It has been shown that the indentation test can be adopted to characterize damage resistance [8], in general, and delamination resistance [9,10], in particular, of composites meant to be used for impact application.

Since the primary performance criteria to assess damage resistance are toughness and damage area, several approaches, such as fibre hybridization [11–15], fabric architecture [16–19] and thermoplastic inclusions [20–22], have been employed to optimize them. However, matrix modification through nanoparticles [23] have showed promising results since both the incipient crack sizes and nanoparticle lie in sub-micron range [24]. Thus, homogeneous presence of nanoparticles in matrix delays the crack onset, owing to superior mechanical properties of nanoparticle, and encounter the crack propagation thereby inducing nano-scale toughness mechanisms [26,27].

A survey of literature shows attempts to investigate optimum nanoparticle content and effect of nanoparticle addition on damage suppression, of carbon and glass fiber composites, under indentation loading as two major themes. For instance, Hoseinlaghab et al. investigated optimum nanoclay content of glass-epoxy composites using quasi-static indentation test [25].Clay content varied at a ratio of 1, 3, 5 and 7 wt. % of epoxy. An improvement in toughness and peak load of 7.4 and 18% was noticed for laminate modified with 3 wt. % of nanoclay when compared to reference sample. Above optimum loading level of nano clay, both toughness and indentation force dropped below reference values. Identically, the projected damage area of 3 wt. % laminate was the lowest among all signifying activation of crack deflection and bowing mechanisms. Lazar et al. modified epoxy with nanosilica at a concentration of 0.5, 0.75, 1 and 3 wt. % to investigate indentation properties of glass fiber composites [26]. Exfoliated structure was corroborated through XRD results, and the damaged samples were analyzed through C-scan to establish relation with nanoparticle concentration. Energy absorption improved by 57.93% at optimum concentration of 0.75 wt. %. However, the highest peak force improvement (39.14%) was noticed for 0.5 wt. % of nanosilica reinforce composites. Rough fracture surfaces induced by nanoparticle debonding, and crack bowing were credited to have increased the failure energy. Identically, damage areas were reduced for nanoparticle reinforced composites.

Almitani et al. incorporated fixed alumina nanoparticle concetration (3 vol. %) in epoxy to fabricate CFRP laminates to be tested for damage resistance under indentation loading [27]. Laminates were indented until controlled displacement values and forwarded for C-scan to calculate damage area. An improvement of 27.5% in damage threshold load was noticed for toughened composites. Nanoparticles were believed to enhance Mode II fracture toughness and interlaminar shear strength thereby delaying damage onset. Tehrani et al. modified epoxy with MWCNT (2 wt. %) to investigate the factors contributing to enhanced performance of CFRP [28]. The punch test confirmed that the toughness level and the damage modes were identical to the high velocity impact test. A high penetration load for nanocomposite indicated retardation of fiber breakage, a feature attributed to improved fiber-matrix load transfer, enhanced shear strength and higher strain to failure. Gao et al. fabricated carbon fiber laminate interleaved with thermoplastic particles to study indentation behavior [29]. Two different areal weights of fiber, 135 and 140 g/m^2, were used with all interlaminar regions modified with 38 μm diameter particles. An improvement of 44.77 and 57.14% in delamination onset energy was noticed for 135 and 140 g/m^2 areal weight composites. Test results corresponded well with improvement noticed in Mode II fracture toughness of identical composites.

An overview of the reported literature shows the potential of MWCNT in enhancing mechanical properties of composites, in general [30]. Several aspects of the effect of functionalized MWCNT addition in glass/epoxy composites, under out of plane loading, have been reported including determining ballistic limit [31,32], optimizing content in pre-stretched condition [33] measuring damage area [34]. However, studies on carbon/epoxy composites were restricted to

Table 1 – Basic features and properties (physical/mechanical) of fibre and matrix (Source: Data Sheet).

Carbon Fibre (Pyrofil$_{TM}$)		Epoxy (HexaMatrix™)	
Characteristic	Value/Description	Characteristic	Value/Description
Fabric Type	Plain Weave	Epoxy: Hardener	100:22
Number of Filaments	3000	Viscosity	1250 ± 250 mPa s
Filament Diameter	7 μm	Density	1.15 g/cm^3
Tensile Strength	4120 MPa	Glass Transition Temperature	80 °C
Tensile Modulus	234 GPa	Tensile Strength	65.33 MPa
Elongation at break	1.8%	Tensile Modulus	2.77 GPa
Density	1.79 g/cm^3	Elongation at break	7.2%

optimizing COOH-MWCNT content, through impact testing, under normal [35] and cryogenic conditions [36]. Another study adopted differently treated MWCNT, at a fix ratio, to report impact properties of carbon composites [37]. Since earlier reported results focused on optimizing the nanoparticle content, in carbon/epoxy composites, as the dominant theme, comprehensive account of MWCNT addition on other damage resistant parameters such as external damage area, damage shape, matrix cracking index and delaminated area is missing. This study reports first comprehensive damage characterisation of amine functionalized MWCNT reinforced carbon composite under quasi-static indentation loading. Indentation loading is significant too, as compared to impact, in characterising the damage sequence together with charting critical interaction of inter and intra-laminar damages through fractography [38–40]. Main contribution lies in investigating effect of different amine functionalized MWCNT concentrations on (i) damage resistance properties and (ii) damage modes and areas. Several toughness parameters such as peak force, displacement, contact stiffness, energy absorption (elastic, plastic and until peak force) and matrix cracking index were correlated to functionalized MWCNT concentration together with a discussion on underlying nano-scale toughness mechanisms. Identically, damage characterisation was done through macrography and ultrasonic c-scan to correlate external damage area and delaminated area, respectively, with MWCNT concentration and toughness.

2. Methodology

2.1. Materials

Aminated multi walled carbon nanotubes (NH_2-MWCNT) were procured from HWNANO (China). Diameter and length ranges were 10–30 nm and 5–15 μm whereas purity and amine content of nanotubes were <95.5% and 3.5 wt. %, respectively. Acetone was procured from Sigma Aldrich (Malaysia) to be used as solvent. Plain weave carbon fibre was purchased from Easy Composites (UK) whereas epoxy was purchased from GRAPHENEST (Portugal). Details of the fibre and resin properties are given in Table 1.

2.2. Sample preparation

2.2.1. Epoxy modification

Sample prep started with dispersing different weight fraction (0.3, 0.6, 0.9 and 1.2 wt. % of epoxy) of NH_2-MWCNT in acetone using probe sonicator (Qsonica, Output Frequency: 20 KHz, Probe Dia: 12.7 mm) with NH_2-MWCNT to acetone weight ratio of 1:70. This was to ensure the breakage of nanotube

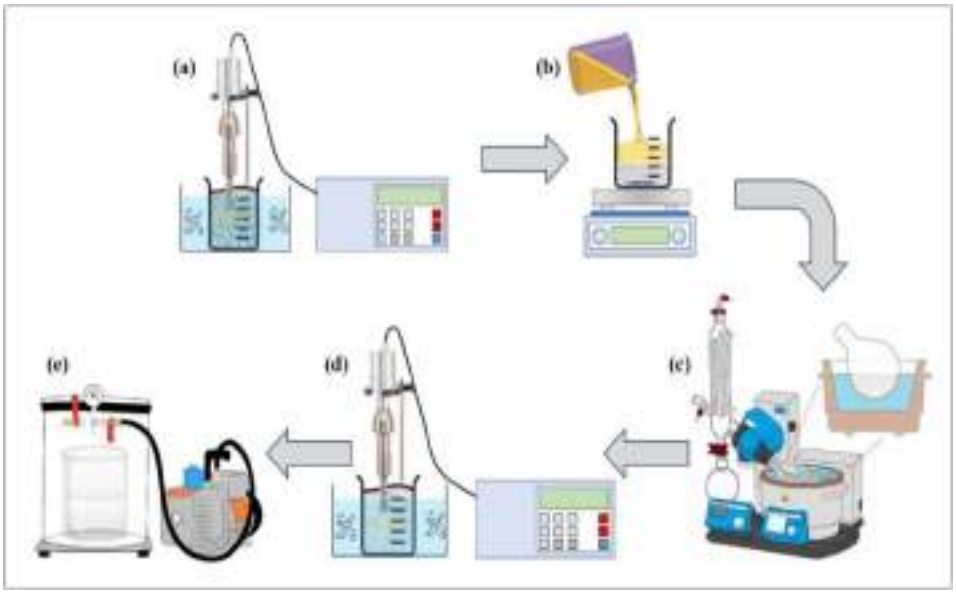

Fig. 1 – (a) NH_2-MWCNT dispersion (b) stirring modified epoxy (c) solvent evaporation (d) modified epoxy sonication and (e) vacuum degassing.

agglomerates prior to mixing it with epoxy. Amplitude, On/Off cycle and sonication time were maintained at 40%, 30s/10s and 20 min, respectively. Following solvent dispersion, initial epoxy weight was added to nanotube suspension to be magnetically stirred (WH240-HT) overnight at 800 rpm. Next, acetone was evaporated (rpm: 100 and Temp: 60 °C) using rotary evaporator (IKA RV10 Auto) adopting acetone module from solvent library. Modified epoxy was sonicated (Amplitude: 40%, On/Off cycle: 1 min/30s) for 30 min in an ice-bath. Maintaining ice-bath helped dissipate the heat generated during sonication [41]. Finally, it was vacuum degassed and mixed with recommended hardener ratio for laminate fabrication. Fig. 1 shows the major steps of epoxy modification.

2.2.2. *Laminate fabrication*

Vacuum bagging technique was employed to fabricate control and NH_2-MWCNT reinforced carbon composites. Fabrication started with preparing mould perimeter and placing a peel ply layer at the bottom of carbon layers. Peel ply was impregnated to ensure that sufficient volume of epoxy pool up and wet the weave texture of fabric. Next, carbon layers were coated with modified epoxy and stacked up to eight layers. Mylar was placed on top of carbon laminate followed by breather fabric. Finally, mould was closed using transparent vacuum bagging film to evacuate the mould of air and allow the laminate to cure for 24 h at room temperature. Sample was demoulded to be placed inside oven for 8 h at 80 °C for post-curing. Next samples were cut into required dimensions for indentation testing. Fibre to matrix volume fraction was calculated to be 0.50:0.48. Fig. 2 presents major steps of laminate preparation.

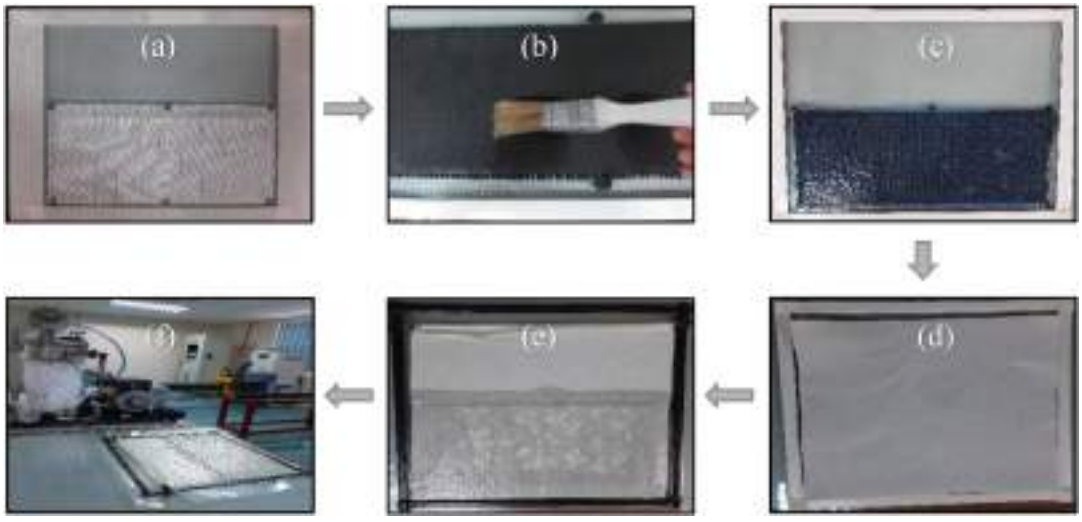

Fig. 2 – (a) Peel ply (b) carbon layers (c) mylar (d) breather fabric (e) bagging film and (f) laminate curing.

3. Characterisation

3.1. *Mechanical characterization*

Quasi-static indentation tests were conducted on universal testing machine (Shimadzu AGS-X). Square samples were placed between the clamping plates and cantered on the origin of the circular unsupported area. Clamping plates were screwed using torque wrench (TOPTUL DT-030S2) with an optimized torque of 10 N m. A hemispherical indenter (Diameter: 9.93 mm) was utilized to induced concentrated force on samples at a crosshead displacement of 1.25 mm/min. Pre-loading of 3 N magnitude was applied prior to running test to ensure effective interaction between indenter and carbon samples. Trapezium X software was used to retrieve force, displacement, and time data until samples were completely penetrated. Four specimen per samples were tested to ensure representative results. Fixture and indenter design, configuration and test parameters were adopted from "Standard Test Method for Measuring the Damage Resistance of a Fibre-Reinforced Polymer-Matrix Composite to a Concentrated Quasi-Static Indentation Force" (ASTM D6264-98). Fig. 3 shows test arrangement and toughness parameters derived from curve.

3.2. *Damage characterisation*

3.2.1. *Fractography*

Samples were cut along the axis coinciding with mid span of damage area and parallel to fibre direction. Cross-sections of damaged faces of samples were scanned using field emission scanning electron microscope (Hitachi SU8020). Samples were processed through platinum sputter coater (Q150R-S) prior to fractography.

3.2.2. *Matrix cracking index*

Quasi-static indentation loading entails matrix cracking as an incipient defect type long before major stiffness loss is noticed on force–displacement curve [40]. Since the noticeable force drop towards the tail end of elastic region of curve signifies the onset of delamination, it is possible to take acoustic data of matrix cracking events through voice recorder and quantitatively analyse it to arrive at another performance criterion i.e., matrix cracking index [42]. A facile approach is to record matrix cracking from the first such instance to the initial force

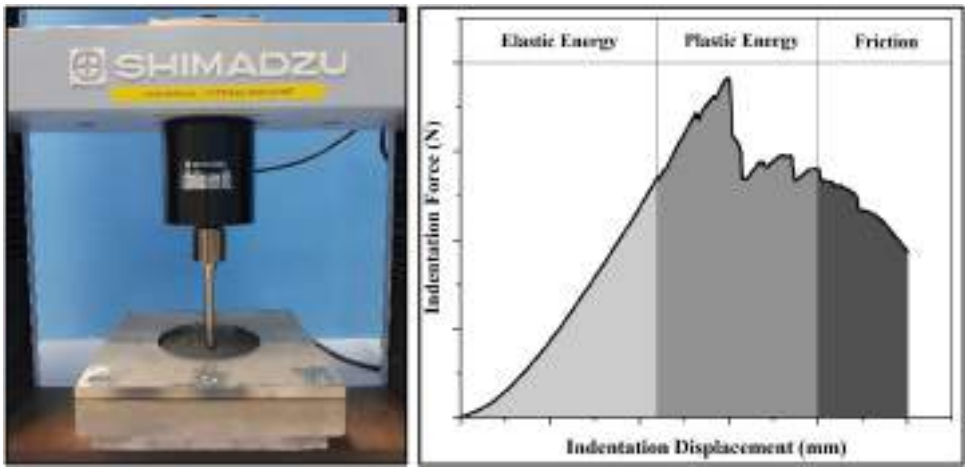

Fig. 3 – (a) Indentation test arrangement (b) major toughness parameters.

drop, an indication of stiffness loss and delamination initiation. Index will be a ratio of the force range, in which matrix cracking data was collected, divided by number of matrix cracking event. A comparable approach has been reported to calculate matrix cracking density by counting matrix crack marks per unit area [43].

Calculation will be as follows:

$$Matrix\ Cracking\ Index = \frac{F_D - F_{MC}}{n}$$

where.

$F_{D:}$ Initial force drop or force at initial stiffness loss.

F_{MC}:Force value at first matrix crack event

n: Number of matrix crack event.

3.2.3. *Macrography*

Macro-shots of external damage area were taken using camera (VIVO X70 PRO) mounted with macro lens (50 MP, f/1.8 (Wide), 1.0 μm). This was to document macro scale damage mechanisms, measuring external damage area and ascertaining damage shapes. For that, three specimens per sample were macro-shot and photographs were processed through image analysis software (Digimizer). This involved calibrating the image followed by measuring damage area using area tool. Damage shape can be quantified through roundness parameter which is calculated by:

$$Roundness = \frac{4\pi A}{P \times P}$$

where.

A:Area.

P: Perimeter.

Roundness will be a value between 0 and 1. Value close to 1 indicate more roundness and 1 is the value for circle.

3.2.4. *Non-destructive inspection*

Samples were analysed through ultrasonic c-scan to detect delaminated area. Twin tower equipment (USL, UK) was operated in automated pulse echo mode to map the projected damage area. Probe capacity, scan index and scanning speed were 5 MHz, 2 mm and 350 mm/s, respectively. All samples were scanned from non-indented side.

4. Results and discussion

4.1. *Force-displacement behaviour*

Force-displacement behaviour of carbon composite showed a steady rise in force value with increment in laminate deformation. All laminate's curves featured linear elastic, peak force and post-peak force plateaued regions. Also, fibre reinforced nanocomposites exhibited a sudden drop in load immediately after peak force value. That indicated at the greater potential of nanocomposites to store energy before catastrophic failure. Additionally, elastic portion of the nanocomposite's curves featured flexing response which started to subside with increment in NH_2-MWCNT concentration. This was owing to emergence of stiffening effect of NH_2-MWCNT at higher concentrations as indicated by contact stiffness (Fig. 4 (f)).

4.2. *Indentation properties*

Peak force and displacement of fibre reinforced nanocomposites improved when compared to control samples results (Fig. 5 (a) and (b)). However, the property increment trend shows an obvious behavioural transition from low NH_2.MWCNT concentration to higher ones. Peak force values were 1897.73, 2232.86, 1994.80, 2199.85 and 2290.07 N for control, 0.3NC, 0.6NC, 0.9NC and 1.2 NC, respectively. This amounted to an improvement of 17.65, 5.11, 15.92 and 20.67% for 0.3NC, 0.6NC, 0.9NC and 1.2NC, respectively. Similarly, peak displacement values were noted to be 5.43, 7.56, 6.07, 6.81 and 6.77 mm for control, 0.3NC, 0.6NC, 0.9NC and 1.2NC, respectively. Improvement in peak displacement was 39.22, 11.78, 25.41 and 24.67% for 0.3NC, 0.6NC, 0.9NC and 1.2NC, respectively. Apparently, load bearing response of fibre reinforced nanocomposite was improved by superior interlaminar shear strength and elongation to failure of modified matrix up to 0.3 wt. % of NH_2-MWCNT content. A comprehensive study reporting influence of NH_2-MWCNT concentration on interlaminar shear strength (ILSS) of woven glass composites concluded that the better interfacial stress transfer, through optimum crosslink density between NH_2-

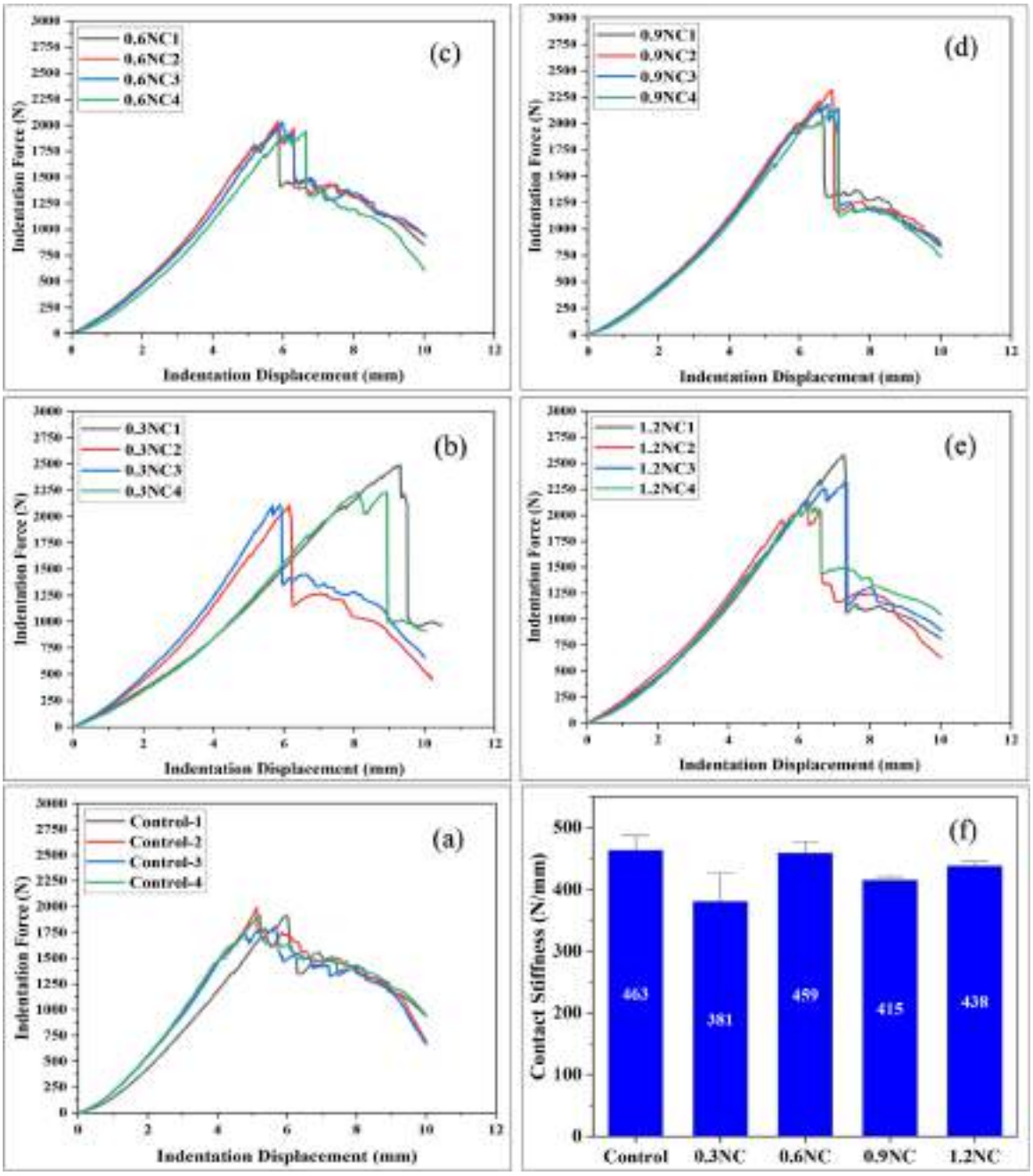

Fig. 4 – Force-displacement curves of (a) Control (b) 0.3 (c) 0.6 (d) 0.9 (e) 1.2 wt. % and (f) contact stiffness of MWCNT reinforced carbon composites.

MWCNT and epoxy, was possible up to 0.3 wt. % of nanoparticle concentration [44]. Another study, utilizing NH_2-MWCNT to investigate its influence on ILSS of woven carbon composites, concluded that ILSS drop above 0.5 wt. % of nanoparticle concentration was due to higher matrix stiffness and extensive interfacial interactions that made interface brittle [45]. Superior elongation to failure resulted from formation of flexible chain segments, owing to epoxy and amine functional group reaction, on interface that would improve stress transfer once interface deform and changes in bond length occur under the external force [46,47].

Above 0.3 wt. % concentration, stiffening effect of NH_2-MWCNT started to dominate (Fig. 5 (b)). In general, peak displacement was higher than that of control sample since elongation at break of NH_2-MWCNT reinforced epoxy has been reported to be superior to pristine epoxy up to 1.4 wt. %. Simultaneously, modulus increases with increment in NH_2-MWCNT loading level in epoxy nanocomposites [48]. Similar behaviour was reported for carbon composites where both elongation and flexural modulus of carbon composites improved up to 1 wt. % of MWCNT loading level. Higher surface area available at higher MWCNT concentration offered desirable stress transfer in interlaminar and intralaminar regions and promoted crack bridging effect [49]. Considering the dispersion quality, agglomerates are reported to be effective too in increasing modulus of the epoxy [50].

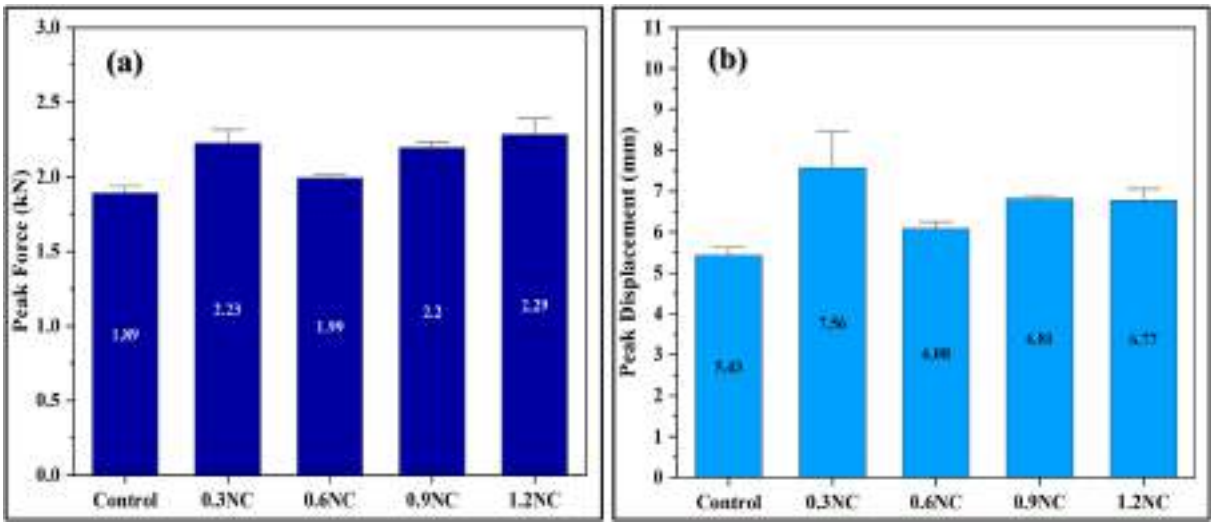

Fig. 5 – (a) Peak force and (b) peak displacement of control and fibre reinforced nanocomposites.

Minor force drops on the elastic portion of the force–displacement curve are associated with matrix cracking induced delamination and consequent stiffness loss of the laminate in quasi-static indentation test [39]. Fig. 6 (a) show an example of typical stiffness loss event on the curve. Fig. 6 (b) presents spectrum of stiffness losses for difference concentrations of NH_2-MWCNT reinforced carbon laminates. It could be appreciated that stiffness loss events were recorded thrice for control samples in force range of 1472.97–1702.44 N. However, this feature was suppressed for low nanoparticle concentration of 0.3NC and 0.6NC. Two stiffness loss events were recorded for 0.3NC and 0.6NC in the force range of 1847.77–2038.82 N and 1633.57–1813.84 N, respectively. Corresponding displacement ranges were 6.09–6.68 mm and 4.94–5.37 mm, respectively (Fig. 6 (c)). This corroborated earlier conclusion that lower concentration of nanoparticle effectively enhanced interlaminar shear strength [44] and improved elongation to failure of modified

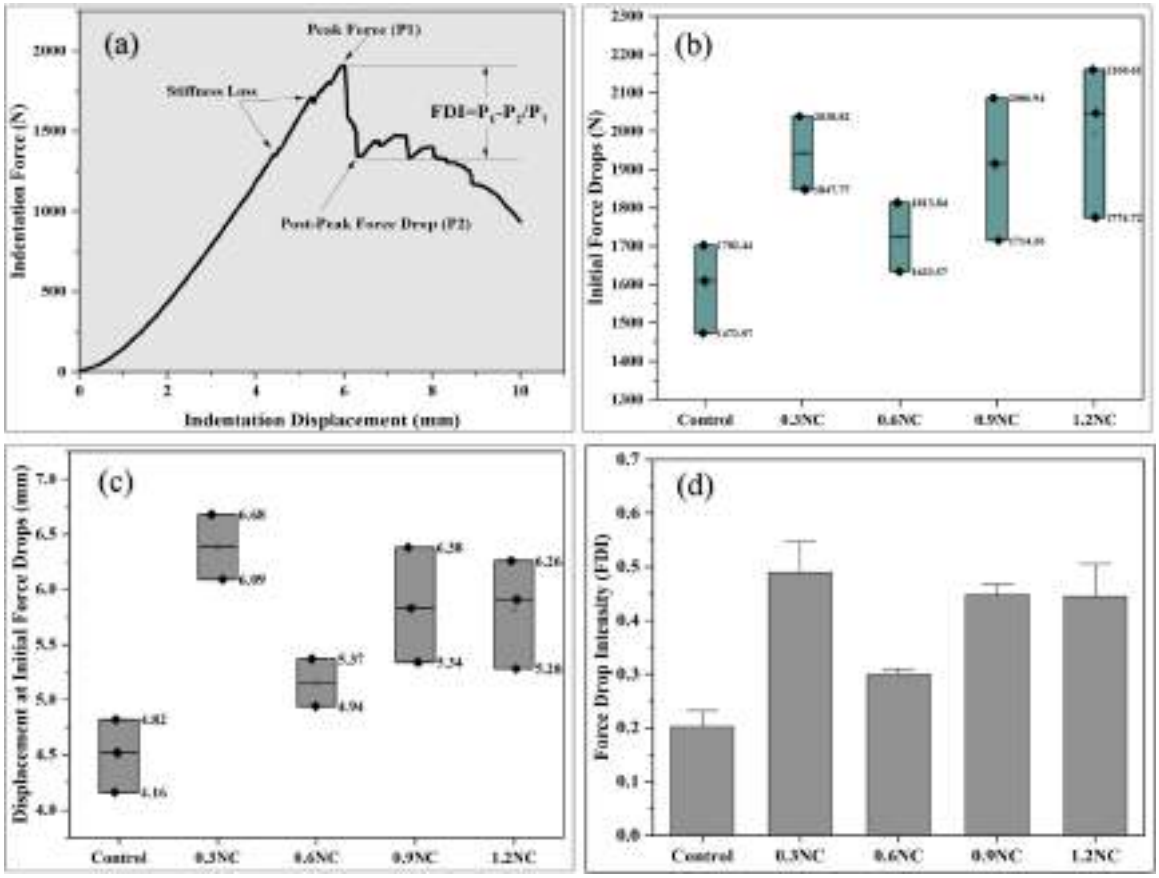

Fig. 6 – . (a) Characteristic stiffness loss and force drop intensity (FDI) features on load–displacement curve and (b) initial force drops (c) displacement at initial force drops and (d) post-peak force drop of fibre reinforced nanocomposites.

matrix. With greater ductility of modified matrix, not only initial matrix cracking was pushed to higher force values but the phenomenon itself was suppressed by interlaminar toughening. Stiff nanoparticles inhibit crack propagation in bulk matrix hence matrix can carry load even after crack initiation [28]. Brittle matrix cracking reappeared at higher nanoparticle loadings, 0.9NC and 1.2NC, as indicated by three major force drops on their force–displacement curves. Force ranges for these were 1714.26–2086.94 N and 1774.72–2160.61 N, respectively. Displacement at force drop ranges were 5.34–6.38 mm and 5.28–6.26 mm for 0.9NC and 1.2NC, respectively. It's worth noting that the force drop ranges for these nanocomposites were much wider and the stiffness loss started at much lower force values when compared to 0.3NC. Effective interaction between NH_2-MWCNT and epoxy added a stiff interface factor into matrix stiffness [51] together with contribution from inherent modulus of nanoparticle to promote crack nucleation and consequent delamination onset/stiffness loss. Additionally, as the mass fraction of interphase increases in the composite system, its properties starts to control the bulk properties especially modulus [47]. Appearance of agglomerates at higher loadings was likely to cause premature matrix cracking too.

Large drop in force after peak-force value is often associated with fibre breakage [39]. Before this stage, however, energy absorption is primarily controlled by out of plane properties of matrix and interface. Hence, magnitude of force drops, after peak-force, can be an indicator of energy absorbing potential of fibre reinforced nanocomposite's microstructure before a performance limiting phenomenon such as fibre breakage happens. This potential can be quantified by force drop intensity (FDI) that is ratio of difference in peak force (P_1) and post-peak force drop value (P_2) and peak force value [52] (Fig. 7 (a)). From this viewpoint, highest force drop intensity was for 0.3NC that exhibited highest improvement in elastic response of laminate and delay in stiffness loss (Fig. 6 (d)). Average values of force drop intensity for control, 0.3NC, 0.6NC, 0.9NC and 1.2NC were 0.2, 0.49, 0.3, 0.44 and 0.44, respectively. Generally, NH_2-MWCNT presence improved the through thickness load transfer by offering effective bonding in interlaminar regions [53]. That might have prevented local buckling of fibre and arrested radial damage growth, hence improving the global deformation response of fibre reinforced nanocomposites. These micro and meso-structural factors allowed the laminates to store greater energy which once released led to a large drop in force values. It's important to note that the highest force drop intensity was often for laminates with superior elastic response which confirm the proposition that force drop, and energy stored in elastic deformation are related (Fig. 7 (a)).

Toughness of the fibre reinforced nanocomposites can be categorized under elastic and plastic zones. This approach helped in identifying the effect of improvement in elastic response, noticed for all concentrations of NH_2-MWCNT reinforced carbon composites, on total energy absorption. Fig. 7 (a) shows the distribution of energy absorption in elastic and plastic phases for different concentrations of nanoparticle reinforced composites together with total energy absorption spectrum. Elastic energy absorption of control, 0.3NC, 0.6NC, 0.9NC and 1.2NC were 2.54, 4.73, 3.3, 3.76 and 3.89 J, respectively. An improvement of 86.22, 29.92, 48.03 and 53.14% were recorded for 0.3NC, 0.6NC, 0.9NC and 1.2NC, respectively. An early stiffness loss, noticed on force–displacement curve, for control samples reduced it to lowest position on elastic toughness scale. This brittle response was replaced with enhanced elastic response of 0.3NC complemented by higher capacity to deform. Plastic toughness values for control, 0.3NC, 0.6NC, 0.9NC and 1.2NC were 6.01, 4.35, 4.8, 4.48 and 4.79 J, respectively. That amounted to reduction of 27.62, 20.13, 25.45 and 20.29% compared to control sample. Roughly, elastic and plastic toughness varied at each other's expense in fibre reinforced nanocomposites. Total energy absorption values for control, 0.3NC, 0.6NC, 0.9NC and 1.2NC were 8.56, 9.06, 8.1, 8.24 and 8.69 J, respectively (Fig. 7 (b)). An improvement of 5.84 and 1.51% were calculated for 0.3NC and 1.2NC, respectively. Toughness dropped for 0.6NC and 0.9NC by 5.3 and 3.73%, respectively.

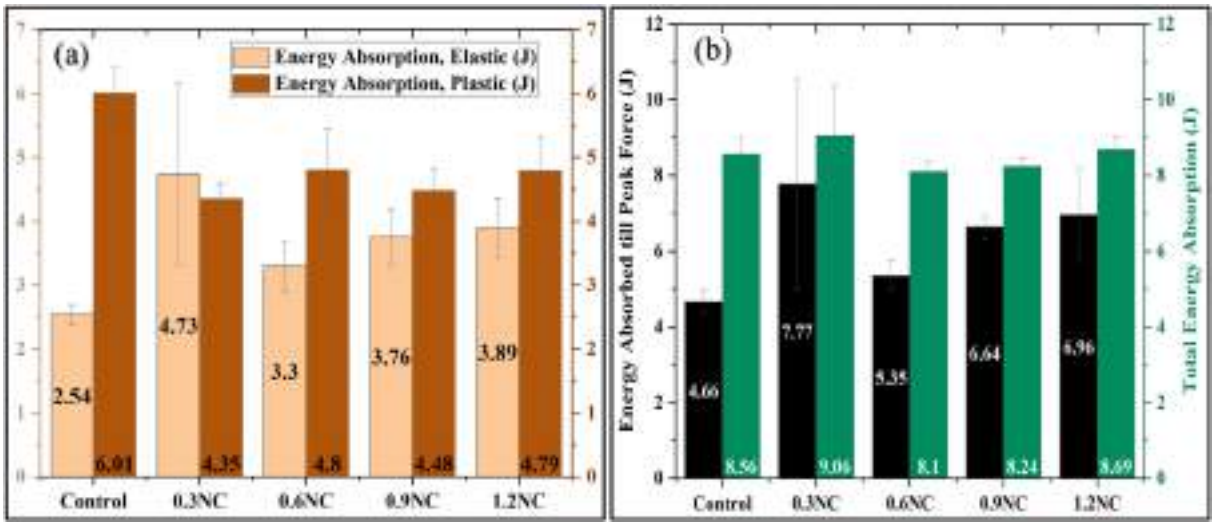

Fig. 7 – (a) Elastic and plastic energy absorption (b) total energy absorption and energy absorption till peak force of fibre reinforced nanocomposites.

Since total toughness of the laminates were calculated up to the last point or plateau on the curve denoting load bearing feature, several factors such as peak force, peak displacement and post-peak force drop influenced total toughness value. Also, elastic response of fibre reinforced nanocomposites was noticed to show improvement, that led to a conclusion to calculate influence of improved elastic response on energy absorption while simultaneously discounting post-peak force factors. A viable parameter to assess that will be to calculate toughness until maximum force. These values were 4.66, 7.77, 5.35, 6.64 and 6.96 J for control, 0.3NC, 0.6NC, 0.9NC, and 1.2NC, respectively (Fig. 7 (b)). An improvement of 66.73, 14.80, 42.48 and 49.35% was noticed for 0.3NC, 0.6NC, 0.9NC and 1.2NC, respectively.

An interplay of two factors seemed to have controlled the toughness of laminates: higher laminate deformation and fracture toughness. At low concentration of 0.3 wt. %, large amount of energy was absorbed in elastically deforming the laminate, a capability offered by improvement in elongation to failure of modified epoxy. In addition, an effective dispersion of NH_2-MWCNT in matrix facilitated covalent bond formation at interface. A reaction ensues between amine functional group of MWCNT and epoxide group involving ring opening and cross-linking. An interlocked structure forms thus which offers impediment to chain mobility in the system [54]. These phenomena retarding delamination and suppressed large scale matrix cracking. However, a transition of response was evident as concentration was increased to 0.6 wt. % and beyond. Laminate deformation capability was reduced and the NH_2-MWCNT concentration started to dictate the properties. Also, TEM observations of NH_2-MWCNT concentration of 0.5 wt. % has been reported to feature agglomerates in microstructure of epoxy [31]. Apparently, reduction in matrix ductility arrested the contribution from elastic deformation of laminate into total energy absorption. However, nanoparticle associated fracture mechanisms became main contributor to toughness of the fibre reinforced nanocomposites. When crack propagates in such a system, an encounter with strong NH_2-MWCNT forces it to stop or change the crack path frequently. Conversely, in case of NH_2-MWCNT pull-out, energy at crack tip reduces significantly [55]. These fracture mechanisms made crack initiation and propagation energy intensive in nanocomposites. Similar, two factor contribution i.e., elastic deformation and fracture toughness into total energy absorption has been reported in case of NH_2-MWCNT reinforced glass fibre composites under impact loading [31].

4.3. *Matrix cracking index*

Kernel smooth curves for matrix cracking of control and fibre reinforced nanocomposites are shown in Fig. 8. Kernel

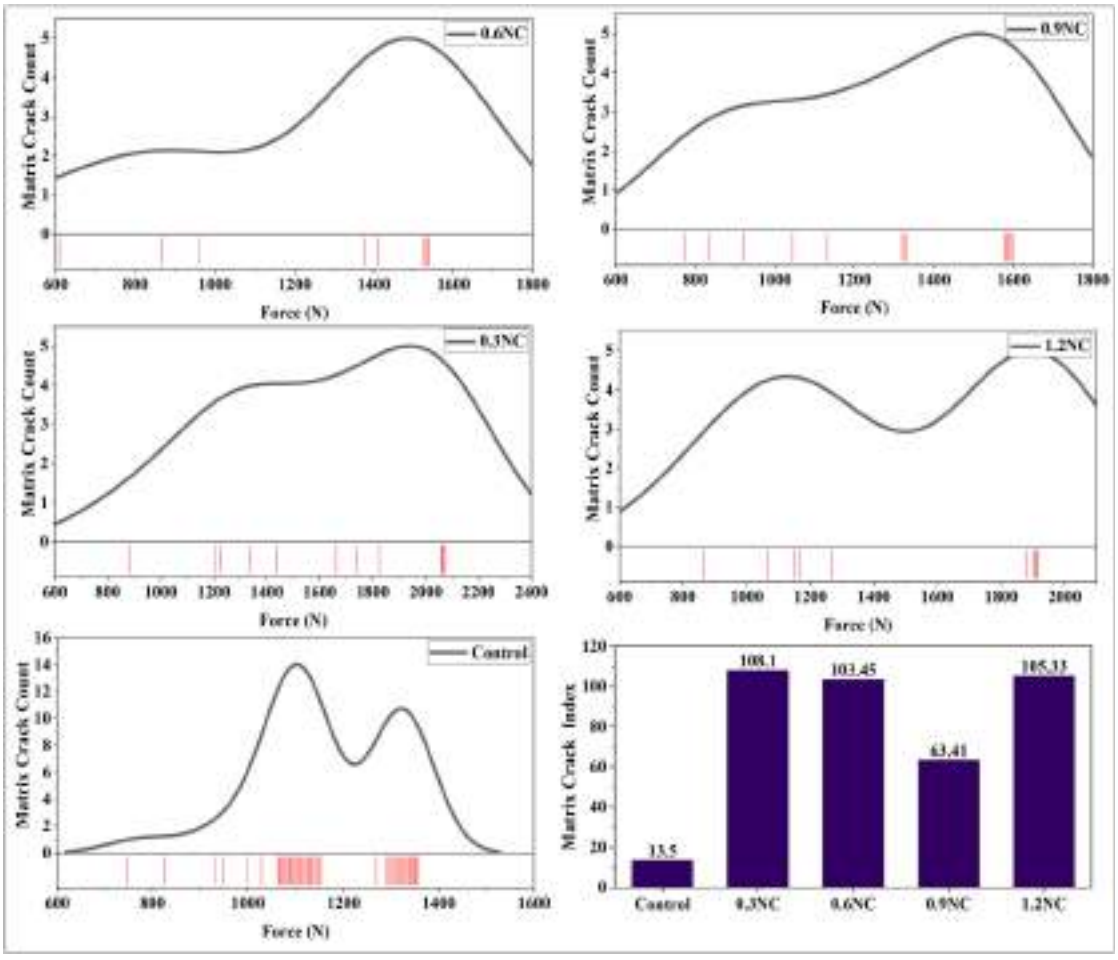

Fig. 8 – Kernel smooth 's curves of matrix cracking event for fibre reinforced nanocomposites along with matrix cracking index.

estimations help in finding probability density functions of a random variable given a finite sample [56]. In other words, it can help identify the intensity of an event within a sub-interval of a pre-defined range. Hence, ranges between 400 N and 2400 N were chosen depending upon scatter of the data for individual samples but with bandwidths of 100 N for all samples.

Acoustic data confirmed matrix cracking to be discrete event until the force reached the value of delamination onset as indicated by clusters (red bars) recorded at higher force values. It can be appreciated that most extensive matrix cracking was recorded for control sample. In general, introduction of nanoparticle suppressed matrix cracking at all concentrations [43]. Also, severity of delamination onset, indicated by clustering of matrix cracking, was reduced with nanoparticle addition. Both extensive crack initiation in bulk matrix and accumulation of cracks appear to contribute to clustering phenomenon. For instance, matrix cracking due to shear contact of indenter precedes matrix cracking owing to tensile stresses in lower part of laminates. Accumulation of these cracks might happen through transverse crack migration under increasing out of plane load [57]. NH_2-MWCNT has been reported to effectively improve fracture toughness of matrix by bridging the cracks or release stresses at crack tip by experiencing pull-out [58]. Additionally, difference in manufacturing and operating temperature induces ply-level thermal residual strains in composites. These strains are linked to increased susceptibility of matrix to crack. MWCNT's have been reported to suppress coefficient of thermal expansion of carbon fibre reinforced composites thus reducing risk of residual strain induced matrix cracking [43].

Total number of matrix crack signals recorded, before first force drop, for control, 0.3NC, 0.6NC, 0.9NC and 1.2NC were 45, 12, 9, 13 and 10, respectively. That amounted to a suppression of 73.33, 80, 71.11 and 77.77% for 0.3NC, 0.6NC, 0.9NC and 1.2NC, respectively. Since NH_2-MWCNT presence in interfacial region was spotted (Fig. 9 (c)), delay in crack onset, greater degree of matrix plastic deformation and higher angle of crack propagation have been reported to be linked to high interfacial fracture toughness under out of plane shear loading [59]. Force ranges, in which matrix cracking happened, were 747.85–1355.78, 881.14–2070.29, 608.47–1539.54, 774.49–1597.89 and 863.64–1917.02 N for control, 0.3NC, 0.6NC, 0.9NC and 1.2NC, respectively. An optimum concentration of 0.3 wt. % NH_2-MWCNT delayed matrix cracking by 17.82%, on force scale, presumably due to improvement in matrix shear strength [60]. An improvement of 3.56 and 15.48% was noticed for 0.9NC and 1.2NC, respectively, whereas decline in the value of the order of 18.63% for 0.6NC was recorded. Apparently, matrix shear strength started to deteriorate beyond 0.3 wt. % of NH_2-MWCNT coupled by inhomogeneity in microstructure. Also, matrix stiffness was likely to improve with nanoparticle concentration. Matrix shear strength had been reported not to improve proportionately with matrix stiffness due to weaker interfacial strength. On the other hand a soft laminate may be expected to undergo higher degree of shear strain and suppress interface failure under shear loading [59].

Matrix cracking indices for control, 0.3NC, 0.6NC, 0.9NC and 1.2NC were 13.5, 108.1, 103.45, 63.41 and 105.33, respectively. Roughly, indices for fibre reinforced nanocomposites were close to one another except an anomalously short force range for 0.9NC in which matrix cracking happened. That was the reason for lower index of 0.9NC although number of matrix cracking were comparable to other samples.

4.4. *Fractography*

Fig. 9 shows the FESEM images of 0.3NC samples with improved fibre matrix adhesion along with fracture toughness mechanisms. Impregnation of fibre tow by epoxy was evident (Fig. 9 (a)) especially at interface signifying an enhanced interaction of fibre and modified matrix. Fig. 9 (b) showed a region sandwiched between two carbon filaments. Good interface bonding and presence of NH_2-MWCNT can be glimpsed in critical resin-rich inter-fibre region. Fibre-matrix interfaces are vulnerable to failure owing to property mismatch, difference in coefficient of thermal expansion and chemical compatibility issues. Also, a crack nucleation in matrix tends to stick to fibre-matrix interface [61]. NH_2-MWCNT served two purposes in these regions: (1) to actively distribute and transfer external stresses to fibre through resin-rich and interface regions thus improving load bearing response (2) to resist crack initiation and propagation hence improving fracture toughness. In this region, NH_2-MWCNT pull-out was active fracture toughness mechanisms with one end of nanotube pulled-out of the matrix.

Fig. 9 (c) shows the surface of carbon fibre with a thin layer of modified epoxy over it. NH_2-MWCNT presence in interface region showed that an interaction of nanoparticle with epoxy was a major factor behind improved performance of 0.3NC. Most of the NH_2-MWCNT could be seen attached to epoxy surface signifying the effective bonding between epoxy and nanotubes. Amine group attached to MWCNT were believed to promote cross-link density at interface hence improving fibre-matrix interface stress transfer efficiency. This too confirmed the dispersion stability of NH_2-MWCNT in epoxy and its ability to migrate to interface region without agglomerating [62]. Also, it's obvious that the fracture surface propagated through reinforced region, as indicated by voids left by NH_2-MWCNT debonding, a feature enhancing fracture toughness of composites. Fig. 9 (d) shows interface failure with epoxy block detached from the fibre. For the fibre on bottom side, interface failure progressed into a deflected crack that eventually fractured the fibre. The interface region just ahead of deflection showed good fibre-matrix bonding and was reinforced by NH_2-MWCNT (Inset). It's likely that the interface failure in a non-reinforced region propagated along the fibre direction until it encountered a region reinforced with NH_2-MWCNT. Presence of high stiffness nanoparticle ahead of crack front forced the crack to change direction and cut through carbon fibre, a phenomenon that required even higher amount of energy and force. Matrix's ability to deflect the cracks and suppress interfacial failure were primary reasons for higher load bearing capacity and elastic toughness of 0.3NC laminate.

Fig. 10 (a) shows extensive matrix cracking in a fibre tow with NH_2-MWCNT embedded in epoxy matrix. Typical toughness mechanisms associated with nanoparticles were not witnessed and many epoxy fragments were found. Similarly, transvers crack propagation through fibre tows was observed featuring extensive fibre fracture (Fig. 10 (b)). Apparently, a drop

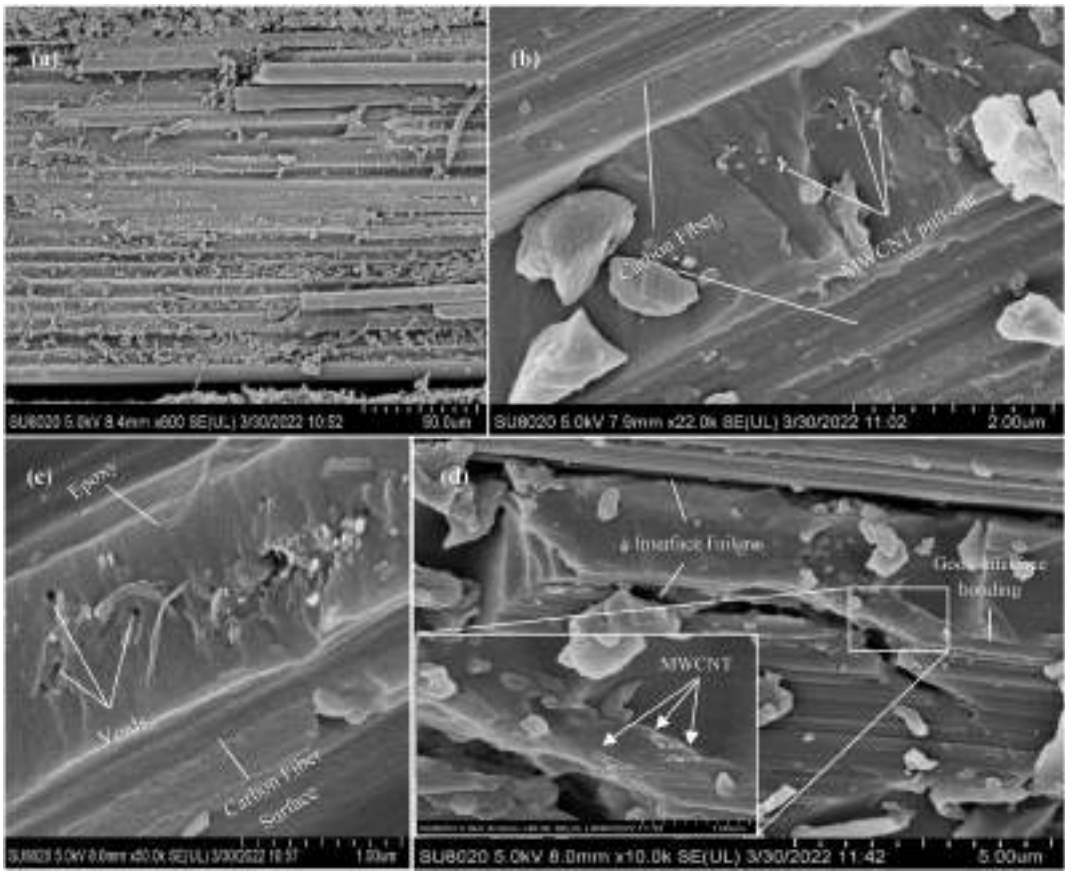

Fig. 9 – (a) Improved fibre matrix adhesion and fracture toughens mechanisms such as (b) MWCNT pull-out (c) voids left by debonding and (d) crack deflection in 0.3NC.

in interlaminar shear strength at 0.6 wt. % of NH_2-MWCNT prompted shear matrix cracking in interlaminar resin-rich regions. These incipient cracks migrated transversely through fibre tows of adjacent ply as the in-plane fracture toughness was high. Load drop was caused presumably by unstable damage growth i.e. transverse cracks accompanied by delamination [57]. Crack migration was accompanied by cutting through fibre under the action of increasing external load.

Higher concentrations of NH_2-MWCNT offered high crosslink density as the degree of interaction between amine functional group of MWCNT and epoxy was expected to offer. Simultaneously, fracture toughness of laminate improved too

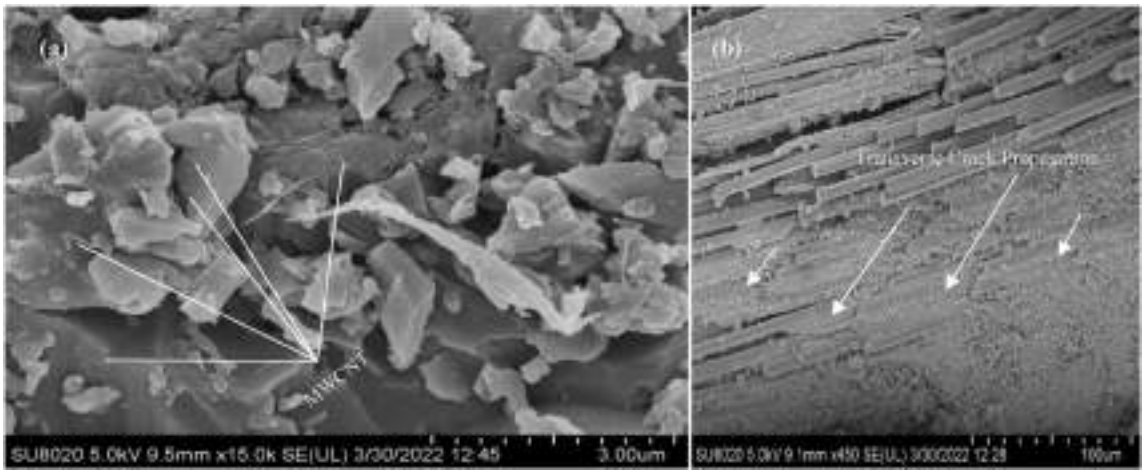

Fig. 10 – (a) Matrix cracking and embedded NH_2-MWCNT and (b) extensive transvers crack propagation in tow for 0.6NC laminate.

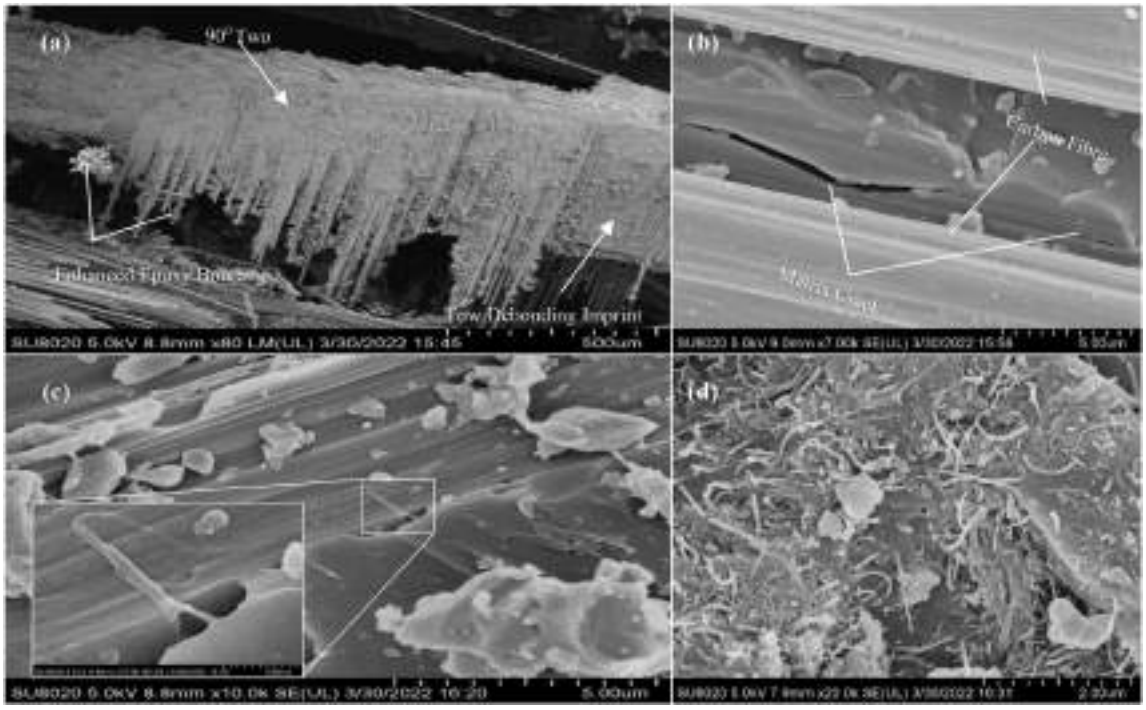

Fig. 11 – (a) Enhanced tow bonding (b) matrix cracking in inter-fibre region (c) crack bridging in 0.9NC and (d) agglomeration in 1.2NC.

since the cracks had to encounter nanoparticle at shorter distances. However, likelihood of negative effect of NH_2-MWCNT stiffness and agglomerate increased at higher nanoparticle concentrations. Both 0.9NC and 1.2 NC laminates boosted higher inter-tow bonding as evidenced in Fig. 11 (a). It shows 90° fibre tow pendent to 0° tow and tow debonding imprint in the vicinity. Apparently, enhanced crosslinking in resin-rich inter-tow regions bonded the tows above and below it and acted as bridge under the action of increasing load [31]. Since the bonding was strong and tough enough to resist crack genesis and propagation, inter-tow region carried the load until the stress reached threshold value of fibre breakage. Since the area featuring tow debonding was directly below the indenter, it required high tensile stresses to detach the 90° fibre tow from 0° one.

Higher nanoparticle loading increases the chances of introducing inhomogeneity in nanocomposites. This microstructural deterioration is featured by presence of agglomerates and non-reinforced regions. Regions devoid of nanoparticles such as inter-fibre zone are susceptible to fracture initiation Fig. 11 (b). Such cracks may be induced by higher shear stress and tensile stresses in upper and lower parts, respectively, of laminate under indentation loading. Cracks originating in brittle matrix region tends to migrate to interfaces hence severely inhibiting load bearing capacity of laminate. However, nanoparticle presence at interface region resists interfacial crack growth and absorb energy thereby. Fig. 11 (c) shows interface crack and its bridging by NH_2-MWCNT. NH_2-MWCNT acted as bridge with one end anchored on a thin layer of epoxy deposited on carbon fibre surface whereas the other end bonded to bulk matrix. Once the interface failure progressed, that bridge fractured on the bulk matrix side while absorbing energy. These nano-scale toughness mechanisms are likely to multiply when the nanoparticle loading increases given the homogeneous dispersion in matrix. On the contrary, agglomerated zone in microstructure (Fig. 11 (d)) not only facilitate premature failure but also degrade the properties by inducing voids and insufficient wetting of reinforcements owing to rise in viscosity. Both types of damage modes, controlled by agglomerated and homogeneously dispersed zones, seemed to be active at higher loading levels and ultimate performance of a specimen, presumably, was dictated by the dominance of one type over the other.

4.5. *Damage characterisation*

4.5.1. *External damage area*

A significant aspect of damage characterisation of composites involves calculating external damage area. Fig. 12 shows macro-shots of external damage area of both control and nanoparticle modified composites. Indentation test often produce petals on the opposite side of indenter contact through a mechanism called shear plugging [63]. Petal-formation follows semi-circular bulge formation, induced by indenter contact, that evolves in pre-peak load stages. Petal formation was more obvious in control sample where quasi-square damage shape offered a glimpse of four equilateral triangular petal's vertices coinciding with centre point of damage. This was facilitated by damage propagation tendency along the tows in all four directions. Moreover, sharpness at the perimeter of damage indicated that the extensive internal damage allowed indenter to displace laminate in out of plane direction to a higher degree. Petal-formation, sharpness, and directional damage growth, in general, were

suppressed in nanoparticle reinforced composites. Damage shape became quasi-circular and sharpness at damage perimeter was moderate.

Macro-scale damage features of control samples were fibre tensile failure, tow splitting and matrix failure in tows indicated by matt appearance [64]. However, bonding in tow's filament improved, for modified composites, together with greater proportion of tows fracturing in ductile manner as indicated by fibrillar appearance of tow cross-section (Fig. 12 (0.3NC)). Tow splitting disappeared completely although tow tensile failure was observed. Another noticeable damage mode of modified composites was appearance of strained tows in the vicinity of damage area. That might be an outcome of greater cohesion among layers, induced by nanoparticle

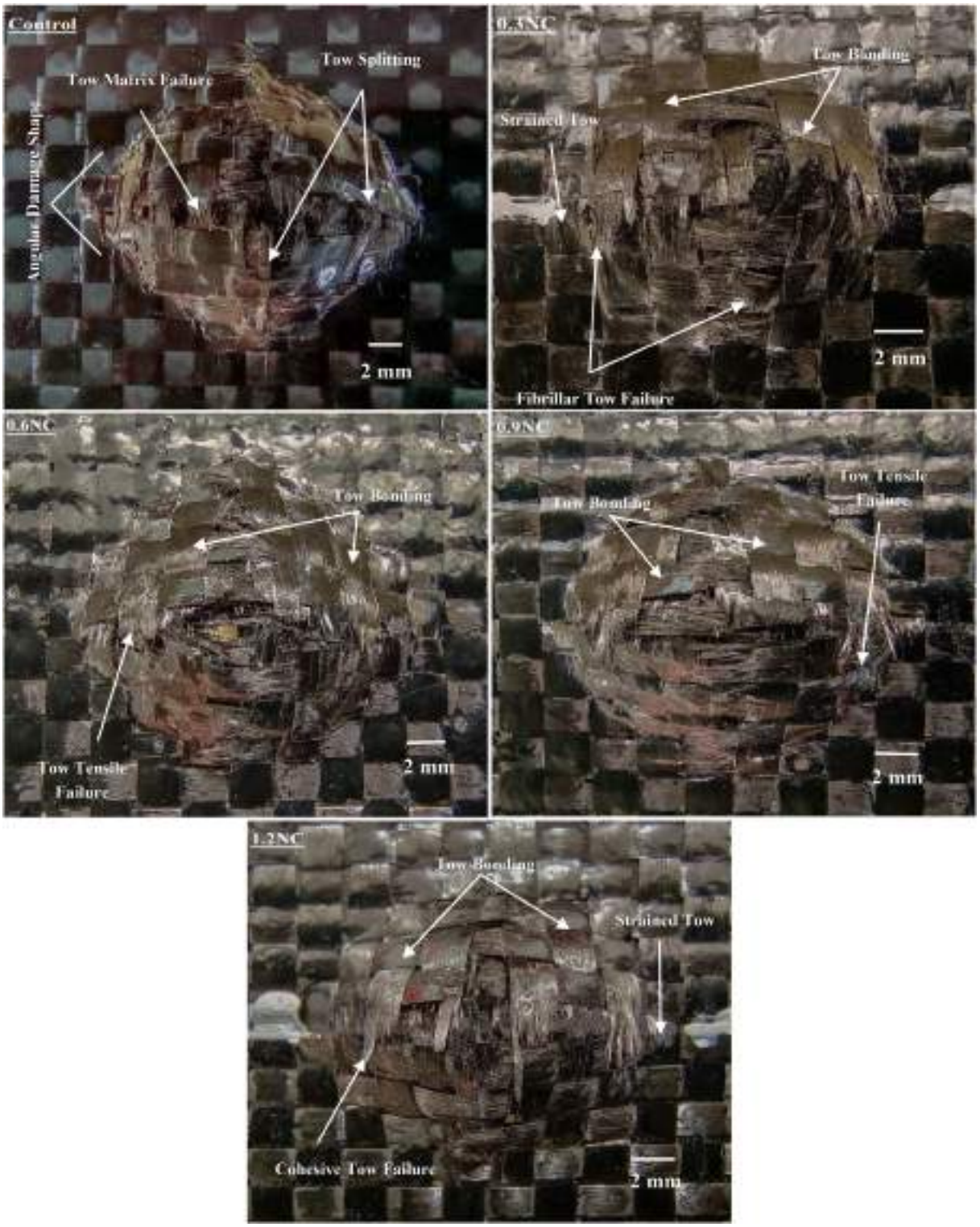

Fig. 12 – External damage of control and NH_2-MWCNT reinforced carbon composites.

presence, that engaged surrounding tow in providing load bearing response.

Damage area characterisation revealed the suppression of damage area at an optimum nanoparticle concentration of 0.3 wt. %. The measured values for control, 0.3NC, 0.6NC, 0.9NC and 1.2NC were 171.18, 143.6, 182.42, 182.93 and 200.1 mm^2, respectively. This amounted to an increment of 6.56, 6.86 and 16.89% for 0.6NC, 0.9NC and 1.2NC, respectively. However, damage area reduced 16.11% for 0.3NC. A higher interlaminar shear strength and matrix ductility suppressed delamination and absorbed energy in elastic deformation, respectively, thus localizing the damage area [31]. In contrast, damage area increased at higher nanoparticle concentration since the higher laminate stiffness (Fig. 4 (f)) reduced deformation capacity and released the absorbed energy in creating internal fracture surface. This was confirmed by correlation of total toughness values with damage area of modified composites (Fig. 13 (a)). 0.3NC laminate absorbed highest amount of energy primarily owing to higher elastic deformation it underwent (Fig. 5 (b)). Damage area and toughness values of 0.6NC and 0.9NC were closed to one another. For 1.2NC, improvement in toughness value led to increment in damage area. Comparison of modified samples with control, along the same line, might not be appropriate as sudden post-peak load drop significantly reduced toughness values of modified composites (Fig. 6 (d)), a factor absents in case of control sample.

Fabric reinforced composites have been reported to exhibit directional growth of damage primarily along fibre orientation [65]. This can be understood to be the tendency of crack to find advancing path along brittle planes on which fibre are located. Propagation of unstable crack growth along brittle planes will severely inhibit load bearing capacity of laminate. Sine this tendency can be indicated by the shape and geometry of external damage area, roundness of damage area can be adopted to indicate the suppression of this tendency in laminates. Fig. 13 (b) presents variation in roundness of damage area for indentation tested laminates. In general, roundness improved with nanoparticle addition. The values were 0.78, 0.9, 0.82, 0.84 and 0.88 for control, 0.3NC, 0.6NC, 0.9NC and 1.2NC, respectively. An improvement of 15.38, 5.12, 7.6 and 12.82% were calculated for 0.3NC, 0.6NC, 0.9NC and 1.2NC, respectively. A higher roundness value was observed to be associated with circle-like shape whereas lower ones with square-like shape. Highest roundness value for 0.3NC seemed to result from superior matrix ductility that allowed greater compliance to indenter contact and localized the damage. However, at higher nanoparticle concentration, superior laminate stiffness distributed the load in the vicinity of contact too presumably owing to improved tow bonding (Fig. 11 (a)).

4.5.2. C-Scan

Delaminated area of carbon composites was mapped through ultrasonic c-scan (Fig. 14). Delamination shape for control sample was square-like with sharp angles at corners. This might stem from the tendency of delamination to propagate along fibre direction as indicated by position of four corners of damage shape. However, this proclivity was suppressed, in general, in NH_2-MWCNT reinforced carbon composites. Damage shape became quasi-circular with mapped contours showing blunt angles. Projected delaminated areas for control, 0.3NC, 0.6NC, 0.9NC and 1.2NC were 238, 242, 200, 172 and 186 mm^2, respectively. 0.3NC showed a marginal increment of 1.68% in delaminated area. However, delaminated was suppressed by 15.96, 27.73 and 21.84% for 0.6NC, 0.9NC and 1.2NC, respectively. Since elastic deformation of 0.3NC was superior to all (Fig. 5 (b)), there was little magnitude of energy left for creating internal fracture surface. This resulted in improvement in toughness while simultaneously restricting the damage value close to that of reference sample. For higher nanoparticle concentrations, significant reduction in delamination was an outcome of nanoparticle induced toughness mechanisms. High surface area to volume ratio NH_2-MWCNT introduces energy absorbing interfaces together with toughness mechanisms such as MWCNT pull-out and fracture (Fig. 9 (b)). Additionally, crack genesis and propagation were arrested both in inter-ply and intra-ply zones due to higher fracture toughness imparted by nanoparticles [66]. A rise in delaminated area value for 1.2NC might be owing to higher than optimum crosslink density, resulting from NH_2-MWCNT and epoxy interaction. This was featured in agglomerated zones (Fig. 11 (d)) that in turn were reducing delamination resistance.

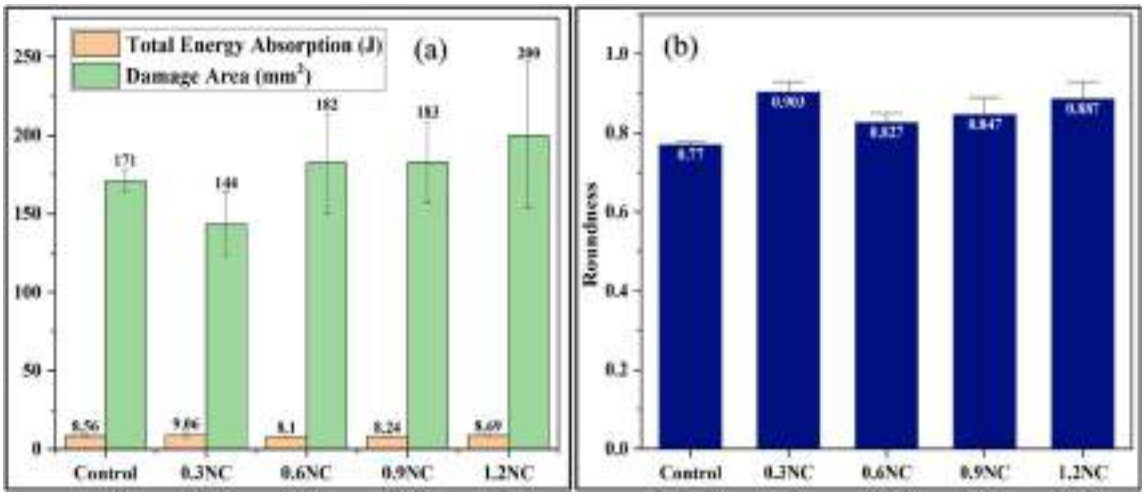

Fig. 13 – (a) Damage area and (b) damage shape roundness of control and NH_2-MWCNT reinforced carbon composites.

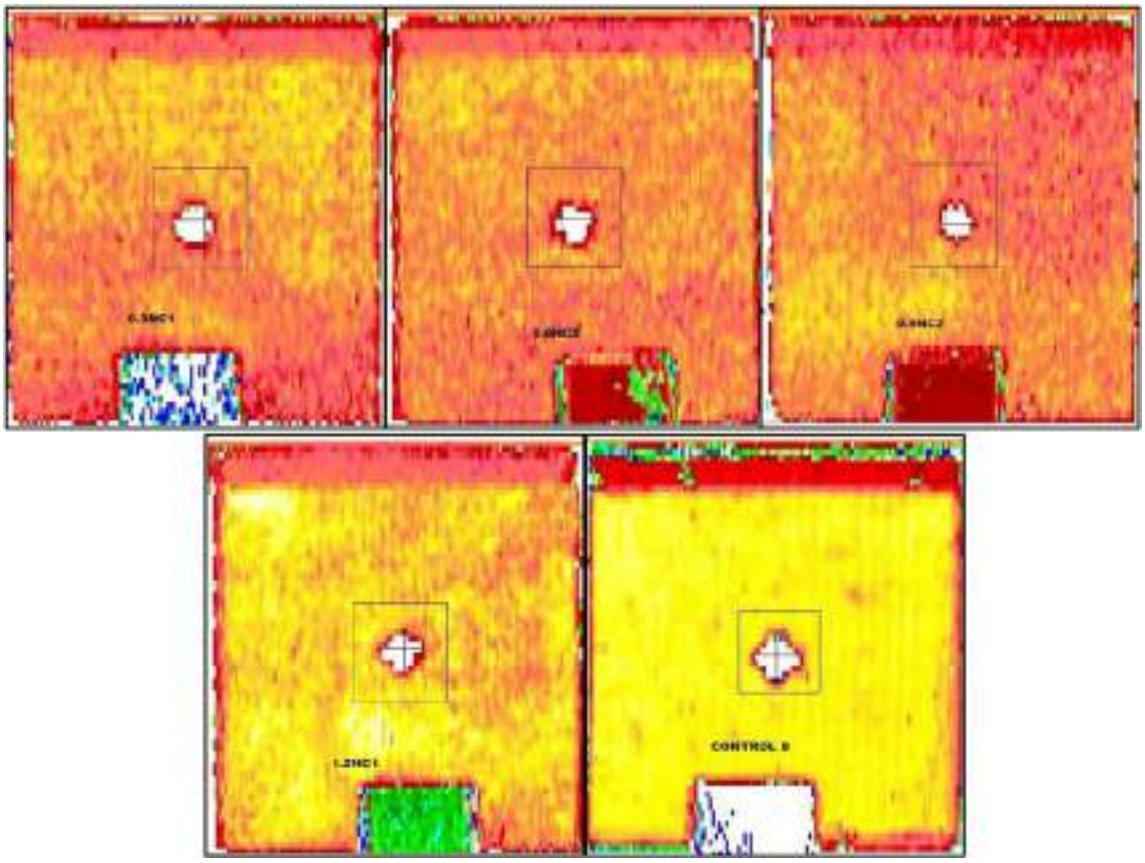

Fig. 14 – C-scan images of fibre reinforced nanocomposites and control samples.

5. Conclusion

This study investigated the effect of amine functionalized MWCNT loading ratio on damage resistance of carbon fibre composites. For that, nanoparticle reinforced epoxy was prepared through solvent dispersion method followed by laminate fabrication using vacuum bagging technique. Laminates were tested under quasi-static indentation loading to assess toughness and load bearing parameters as they vary with NH_2-MWCNT concentration. Elastic deformation and toughness improved significantly at low NH_2-MWCNT concentration (0.3NC). At higher concentrations (0.6NC, 0.9NC and 1.2 NC), higher laminate stiffness offered superior load bearing response. Matrix cracking was suppressed significantly at all NH_2-MWCNT concentrations. Fractography revealed higher fibre-matrix adhesion, tow bonding and nano-scale toughness mechanisms such as nanoparticle pull-out, crack deflection and bridging. External damage area reduced at lowest concentration (0.3NC) then rose steadily with nanoparticle concentration. Delaminated area reduced, generally, for all fibre reinforced nanocomposites although a nominal increment was noticed at lowest concentration (0.3NC). From the materials design perspective, future works may focus on optimizing cross-link density of NH_2-MWCNT-epoxy nanocomposites by varying amine content on nanoparticles. This will help avoid negative consequences of high cross-link density at higher NH_2-MWCNT loading levels. As for damage characterisation, a ply-by-ply study of the delaminated area will be helpful in procuring a holistic picture of the influence of nanoparticle on delamination resistance of composites. Future works along theses frontiers will not only offer novel insights about fibre reinforced nanocomposites but also increase their potential in wider structural applications.

Author's contribution

Usaid Ahmed Shakil: Conceptualization, experimentation and writing.
Shukur bin Abu Hassan: Funding and Supervision.
Mohd Yazid bin Yahya: Supervision.
All authors reviewed the manuscript.

Data availability statement

The raw/processed data required to reproduce these findings cannot be shared at this time as the data also forms part of an ongoing study.

Declaration of Competing Interest

The authors declare that they have no known competing financial interests or personal relationships that could have appeared to influence the work reported in this paper.

Acknowledgment

First author would like to thank Higher Education Commission, Pakistan for the award of study scholarship. Authors would like to thank Universiti Teknologi Malaysia to provide monetary assistance through grant number Q.J091600.3100.00A37 (Dana Universiti Penyelidikan) for carrying out this work. Also, authors are grateful to Universiti Malaysia Pahang to finance this research through grant number PGRS210340.

REFERENCES

[1] Soutis C. Fibre reinforced composites in aircraft construction. Prog Aero Sci 2005;41(2):143–51.
[2] Kim J-K, Mai Y-W. High strength, high fracture toughness fibre composites with interface control—a review. Compos Sci Technol 1991;41(4):333–78.
[3] Feih S, Wei J, Kingshott P, Sørensen BF. The influence of fibre sizing on the strength and fracture toughness of glass fibre composites. Compos Part A Appl Sci Manuf 2005;36(2):245–55.
[4] Mahmood AS, Summerscales J, James MN. Resin-rich volumes (RRV) and the performance of fibre-reinforced composites: a review. J Compos Sci 2022;6(2):53.
[5] Naya F, Pappas G, Botsis J. Micromechanical study on the origin of fiber bridging under interlaminar and intralaminar mode I failure. Compos Struct 2019;210:877–91.
[6] Saeedifar M, Zarouchas D. Damage characterization of laminated composites using acoustic emission: a review. Compos Part B Eng 2020;195:108039.
[7] Gliszczynski A, Kubiak T, Rozylo P, Jakubczak P, Bieniaś J. The response of laminated composite plates and profiles under low-velocity impact load. Compos Struct 2019;207:1–12.
[8] Nettles AT, Douglas MJ. A comparison of quasi-static indentation to low-velocity impact. 2000.
[9] Kaczmarek H, Maison S. Comparative ultrasonic analysis of damage in CFRP under static indentation and low-velocity impact. Compos Sci Technol 1994;51(1):11–26.
[10] Bozkurt MO, Coker D. In-situ investigation of dynamic failure in [05/903] s CFRP beams under quasi-static and low-velocity impact loadings. Int J Solid Struct 2021;217:134–54.
[11] Hajiha H, Sain M. High toughness hybrid biocomposite process optimization. Compos Sci Technol 2015;111:44–9.
[12] Yahaya R, Sapuan S, Jawaid M, Leman Z, Zainudin E. Quasi-static penetration and ballistic properties of kenaf–aramid hybrid composites. Mater Des 2014;63:775–82.
[13] Petrucci R, Santulli C, Puglia D, Nisini E, Sarasini F, Tirillò J, et al. Impact and post-impact damage characterisation of hybrid composite laminates based on basalt fibres in combination with flax, hemp and glass fibres manufactured by vacuum infusion. Compos Part B Eng 2015;69:507–15.
[14] Sarasini F, Tirillò J, D'Altilia S, Valente T, Santulli C, Touchard F, et al. Damage tolerance of carbon/flax hybrid composites subjected to low velocity impact. Compos Part B Eng 2016;91:144–53.
[15] Bandaru AK, Patel S, Sachan Y, Alagirusamy R, Bhatnagar N, Ahmad S. Low velocity impact response of 3D angle-interlock Kevlar/basalt reinforced polypropylene composites. Mater Des 2016;105:323–32.
[16] Atas C, Sayman O. An overall view on impact response of woven fabric composite plates. Compos Struct 2008;82(3):336–45.
[17] Schrauwen B, Peijs T. Influence of matrix ductility and fibre architecture on the repeated impact response of glass-fibre-reinforced laminated composites. Appl Compos Mater 2002;9(6):331–52.
[18] Vieille B, Casado VM, Bouvet C. Influence of matrix toughness and ductility on the compression-after-impact behavior of woven-ply thermoplastic-and thermosetting-composites: a comparative study. Compos Struct 2014;110:207–18.
[19] Yokozeki T, Kuroda A, Yoshimura A, Ogasawara T, Aoki T. Damage characterization in thin-ply composite laminates under out-of-plane transverse loadings. Compos Struct 2010;93(1):49–57.
[20] Cicala G, Mannino S, Cozzo G, Latteri A. Novel polymeric systems for high performance liquid molding technologies. Recent Res Dev Polym Sci 2012;11:77–97.
[21] Shakil UA, Abu Hassan SB, Yahya MY, Rejab MRM. A focused review of short electrospun nanofiber preparation techniques for composite reinforcement. Nanotechnol Rev 2022;11(1):1991–2014.
[22] Shakil UA, Hassan SBA, Yahya MY, Nauman S. Mechanical properties of electrospun nanofiber reinforced/interleaved epoxy matrix composites—a review. Polym Compos 2020;41(6):2288–315.
[23] Shakil UA, Hassan SBA, Yahya MY, Nurhadiyanto D. A review of properties and fabrication techniques of fiber reinforced polymer nanocomposites subjected to simulated accidental ballistic impact. Thin-Walled Struct 2021;158:107150.
[24] Zhang L, De Greef N, Kalinka G, Van Bilzen B, Locquet J-P, Verpoest I, et al. Carbon nanotube-grafted carbon fiber polymer composites: damage characterization on the micro-scale. Compos Part B Eng 2017;126:202–10.
[25] Hoseinlaghab S, Farahani M, Safarabadi M. Improving the impact resistance of the multilayer composites using nanoparticles. Mech Base Des Struct Mach 2021:1–17.
[26] Lazar PJL, Sengottuvelu R, Natarajan E. Assessments of secondary reinforcement of epoxy matrix-glass fibre composite laminates through nanosilica (SiO2). Materials 2018;11(11):2186.
[27] Almitani K, Wagih A, Melaibari A, Eltaher M. Improving energy dissipation and damage resistance of CFRP laminates using alumina nanoparticles. Plast, Rubber Compos 2019;48(5):208–17.
[28] Tehrani M, Boroujeni A, Hartman T, Haugh T, Case S, Al-Haik M. Mechanical characterization and impact damage assessment of a woven carbon fiber reinforced carbon nanotube–epoxy composite. Compos Sci Technol 2013;75:42–8.
[29] Gao F, Jiao G, Lu Z, Ning R. Mode II delamination and damage resistance of carbon/epoxy composite laminates interleaved with thermoplastic particles. J Compos Mater 2007;41(1):111–23.
[30] Nurazzi N, Sabaruddin F, Harussani M, Kamarudin S, Rayung M, Asyraf M, et al. Mechanical performance and applications of cnts reinforced polymer composites—a review. Nanomater 2021;11(9):2186.
[31] Rahman M, Hosur M, Zainuddin S, Vaidya U, Tauhid A, Kumar A, et al. Effects of amino-functionalized MWCNTs on ballistic impact performance of E-glass/epoxy composites using a spherical projectile. Int J Impact Eng 2013;57:108–18.
[32] Eslami-Farsani R, Shahrabi-Farahani A. Improvement of high-velocity impact properties of anisogrid stiffened composites by multi-walled carbon nanotubes. Fibers Polym 2017;18(5):965–70.
[33] Zhang X, Wang P, Neo H, Lim G, Malcolm AA, Yang E-H, et al. Design of glass fiber reinforced plastics modified with CNT

and pre-stretching fabric for potential sports instruments. Mater Des 2016;92:621–31.
[34] Khosravi H, Eslami-Farsani R. High-velocity impact properties of multi-walled carbon nanotubes/E-glass fiber/epoxy anisogrid composite panels. J Comput Appl Res Mech Eng 2020;9(2):235–43.
[35] El Moumen A, Tarfaoui M, Lafdi K, Benyahia H. Dynamic properties of carbon nanotubes reinforced carbon fibers/epoxy textile composites under low velocity impact. Compos Part B Eng 2017;125:1–8.
[36] Kara M, Kırıcı M, Tatar AC, Avcı A. Impact behavior of carbon fiber/epoxy composite tubes reinforced with multi-walled carbon nanotubes at cryogenic environment. Compos Part B Eng 2018;145:145–54.
[37] Siegfried M, Tola C, Claes M, Lomov SV, Verpoest I, Gorbatikh L. Impact and residual after impact properties of carbon fiber/epoxy composites modified with carbon nanotubes. Compos Struct 2014;111:488–96.
[38] Wagih A, Maimí P, Blanco N, Costa J. A quasi-static indentation test to elucidate the sequence of damage events in low velocity impacts on composite laminates. Compos Part A Appl Sci Manuf 2016;82:180–9.
[39] Wagih A, Maimí P, González E, Blanco N, de Aja JS, De La Escalera F, et al. Damage sequence in thin-ply composite laminates under out-of-plane loading. Compos Part A Appl Sci Manuf 2016;87:66–77.
[40] Abisset E, Daghia F, Sun X, Wisnom MR, Hallett SR. Interaction of inter-and intralaminar damage in scaled quasi-static indentation tests: Part 1–Experiments. Compos Struct 2016;136:712–26.
[41] Gkikas G, Barkoula N-M, Paipetis A. Effect of dispersion conditions on the thermo-mechanical and toughness properties of multi walled carbon nanotubes-reinforced epoxy. Compos Part B Eng 2012;43(6):2697–705.
[42] Shakil UA, Abu Hassan S, Yahya MY. Electrospun short nanofibers to improve damage resistance of carbon fiber composites. Polym Compos 2023;44(4):2305–21.
[43] Yokozeki T, Iwahori Y, Ishiwata S. Matrix cracking behaviors in carbon fiber/epoxy laminates filled with cup-stacked carbon nanotubes (CSCNTs). Compos Part A Appl Sci Manuf 2007;38(3):917–24.
[44] Rahman M, Zainuddin S, Hosur M, Robertson C, Kumar A, Trovillion J, et al. Effect of NH2-MWCNTs on crosslink density of epoxy matrix and ILSS properties of e-glass/epoxy composites. Compos Struct 2013;95:213–21.
[45] Sharma VK. Influence of amine functionalized multi-walled carbonnanotubes on the mechanical properties of carbonfiber/epoxy composites. Mater Today Proc 2021;37:2978–81.
[46] Wang S, Liang Z, Liu T, Wang B, Zhang C. Effective amino-functionalization of carbon nanotubes for reinforcing epoxy polymer composites. Nanotechnol 2006;17(6):1551.
[47] Chen W, Lu H, Nutt SR. The influence of functionalized MWCNT reinforcement on the thermomechanical properties and morphology of epoxy nanocomposites. Compos Sci Technol 2008;68(12):2535–42.
[48] Cui L-J, Wang Y-B, Xiu W-J, Wang W-Y, Xu L-H, Xu X-B, et al. Effect of functionalization of multi-walled carbon nanotube on the curing behavior and mechanical property of multi-walled carbon nanotube/epoxy composites. Mater Des 2013;49:279–84.
[49] Mirsalehi SA, Youzbashi AA, Sazgar A. Enhancement of out-of-plane mechanical properties of carbon fiber reinforced epoxy resin composite by incorporating the multi-walled carbon nanotubes. SN Appl Sci 2021;3(6):1–12.
[50] Song YS, Youn JR. Influence of dispersion states of carbon nanotubes on physical properties of epoxy nanocomposites. Carbon 2005;43(7):1378–85.
[51] Khare KS, Khabaz F, Khare R. Effect of carbon nanotube functionalization on mechanical and thermal properties of cross-linked epoxy–carbon nanotube nanocomposites: role of strengthening the interfacial interactions. ACS Appl Mater Interfaces 2014;6(9):6098–110.
[52] Bhudolia SK, Gohel G, Joshi SC, Leong KF. Quasi-static indentation response of core-shell particle reinforced novel nccf/elium® composites at different feed rates. Compos Commun 2020;21:100383.
[53] Mahdi TH, Islam ME, Hosur MV, Jeelani S. Low-velocity impact performance of carbon fiber-reinforced plastics modified with carbon nanotube, nanoclay and hybrid nanoparticles. J Reinforc Plast Compos 2017;36(9):696–713.
[54] Rahman M, Zainuddin S, Hosur M, Malone J, Salam M, Kumar A, et al. Improvements in mechanical and thermo-mechanical properties of e-glass/epoxy composites using amino functionalized MWCNTs. Compos Struct 2012;94(8):2397–406.
[55] Rahman MM, Hosur M, Zainuddin S, Jajam KC, Tippur HV, Jeelani S. Mechanical characterization of epoxy composites modified with reactive polyol diluent and randomly-oriented amino-functionalized MWCNTs. Polym Test 2012;31(8):1083–93.
[56] Mourão MF, Braga AC, Oliveira PN. Smoothing kernel estimator for the ROC curve-simulation comparative study. In: International conference on computational science and its applications. Springer; 2013. p. 573–84.
[57] Aoki Y, Suemasu H, Ishikawa T. Damage propagation in CFRP laminates subjected to low velocity impact and static indentation. Adv Compos Mater 2007;16(1):45–61.
[58] Lachman N, Wagner HD. Correlation between interfacial molecular structure and mechanics in CNT/epoxy nano-composites. Compos Part A Appl Sci Manuf 2010;41(9):1093–8.
[59] Yuan K, Liu K, Zhao M, Wei K, Wang Z. The in situ matrix cracking behavior in cross-ply laminates under out-of-plane shear loading. Compos Struct 2022:115563.
[60] Sydlik SA, Lee J-H, Walish JJ, Thomas EL, Swager TM. Epoxy functionalized multi-walled carbon nanotubes for improved adhesives. Carbon 2013;59:109–20.
[61] Singh DK, Vaidya A, Thomas V, Theodore M, Kore S, Vaidya U. Finite element modeling of the fiber-matrix interface in polymer composites. J Compos Sci 2020;4(2):58.
[62] Zhang Q, Wu J, Gao L, Liu T, Zhong W, Sui G, et al. Dispersion stability of functionalized MWCNT in the epoxy–amine system and its effects on mechanical and interfacial properties of carbon fiber composites. Mater Des 2016;94:392–402.
[63] Sirichantra J, Ogin S, Jesson D. The use of a controlled multiple quasi-static indentation test to characterise through-thickness penetration of composite panels. Compos Part B Eng 2012;43(2):655–62.
[64] Rahman MM, Hosur M, Hsiao K-T, Wallace L, Jeelani S. Low velocity impact properties of carbon nanofibers integrated carbon fiber/epoxy hybrid composites manufactured by OOA–VBO process. Compos Struct 2015;120:32–40.
[65] Habibi M, Abbassi F, Laperrière L. Quasi-static indentation and acoustic emission to analyze failure and damage of bio-composites subjected to low-velocity impact. Compos Part A Appl Sci Manuf 2022;158:106976.
[66] Karapappas P, Vavouliotis A, Tsotra P, Kostopoulos V, Paipetis A. Enhanced fracture properties of carbon reinforced composites by the addition of multi-wall carbon nanotubes. J Compos Mater 2009;43(9):977–85.